Hindawi
International Journal of Antennas and Propagation
Volume 2023, Article ID 5537962, 9 pages
https://doi.org/10.1155/2023/5537962

Research Article

Integrated Design of Multimode and Multifrequency Miniaturized Handset Antenna at VHF/UHF Bands

Yandong Zhang,[1] **Hui Zhang**,[2,3,4] **Liang Xu**,[5] **Linao Li**,[1] **Chunxiao Li**,[5] **and Zhijuan An**[5]

[1]*School of Electronic Engineering, Xi'an University of Posts and Telecommunications, Xi'an 710121, China*
[2]*Chongqing University, Chongqing 400044, China*
[3]*Chongqing Institute of Green and Intelligent Technology, Chinese Academy of Sciences, Chongqing 400714, China*
[4]*Xi'an Starnet Antenna Technology Co., Ltd., Xi'an, China*
[5]*School of Physics, Xidian University, Xi'an 710071, China*

Correspondence should be addressed to Yandong Zhang; 1953035868@qq.com

Received 30 November 2022; Revised 14 January 2023; Accepted 17 January 2023; Published 27 January 2023

Academic Editor: Flaminio Ferrara

This paper presents an integrated design of a multimode and multifrequency miniaturized handset antenna working at the lower band (0.24–0.7 GHz) with linear polarization and higher band (1.98–2.01 GHz and 2.17–2.20 GHz) with circular polarization simultaneously. At the higher band, the quadrifilar helix antenna (QHA) is utilized with each arm developed into two arms of different lengths and linearly tapered widths to realize double resonance and increase the bandwidth. Moreover, a helical stub behaving as a director is introduced to improve the antenna gain. At the lower band, the outer conductor of the QHA feedline and four QHA arms are designed to constitute a monopole antenna through proper feeding and introducing four quarter-wavelength short-circuit stubs. With this radiator-sharing technique, the QHA not only works at the higher band with a circular polarization pattern but can act as a monopole antenna working at the lower band with a linear polarization pattern simultaneously. As a result, the size of the antenna can be reduced remarkably. Finally, the proposed antenna is fabricated with a total length of 228 mm and a diameter of 15 mm. At the lower band, the measured S11 is below −8 dB, and the gain is larger than 0.5 dBi. At the higher band, the measured S11 and AR are better than −13 dB and 3 dB, respectively, and the gain within the zenith angle range of 0°−35° is greater than 2.5 dBi, which demonstrates better performance.

1. Introduction

With the fast development of communication techniques, multimode terminals integrated with multiple functions such as LTE, self-organizing network, intercom, and satellite communication have been widely used; correspondingly, it is required to design the antennas operating at VHF/UHF bands with different modes to realize the aforementioned functions.

At the VHF band and lower band of UHF, the monopole antenna or dipole antenna is often utilized to achieve omnidirectional radiation on the horizontal plane with linear polarization. In [1], two compact monopole antennas working at 149 MHz and 398 MHz are proposed by using meander-line and foldable structures. Das and Iyer [2] proposed a highly miniaturized 3-D spherical folded dipole antenna working at 515 MHz, which employs a spherical helix structure and hence has a very compact structure with a vertical size of only 1/175 of wavelength. However, both the aforementioned two antennas work with a narrower bandwidth. At the higher band of UHF, the quadrifilar helix antenna (QHA) becomes a preferable candidate due to its wide beamwidth and good circular polarization characteristics. In [3], a dual-band QHA is presented, each arm of which consists of two parallel elements with different lengths to achieve double resonance. Byun et al. [4] proposed another kind of dual-band QHA by using stepped-width arms, which can reduce the antenna size and adjust the frequency

interval for dual-band operation. In [5], a low-profile dual-band QHA is proposed by loading the circular metal strips on the dual-helix metal strips with different lengths. In [6], a compact triple-band circularly polarized QHA is designed by the incorporation of a UHF-band QHA and an L/S-band QHA assembled in a "piggyback" fashion.

To realize the integration of multiple functions, it is required to use the multimode and multifrequency antenna to satisfy the multiservice requirement of terminals. Multimode and multifrequency can be achieved by loading slots, stubs, and parasitic elements [7–11], which has the advantages of small size and easy feeding, but often results in pattern distortion or beam splitting. The other way is to use separate antennas arranged side by side or embedded for each band and mode [12–15]. In this way, the antennas should be arranged skillfully to reduce the mutual coupling and the size of antennas as much as possible. However, so far, researches on multimode and multifrequency antennas are mainly concentrated in the fields of GSM, WLAN, WiMAX, GPS, and BDS, etc., and there is very little literature on handset terminal antennas working in the VHF/UHF band. In [16], a folded quadrifilar helix antenna colocated with a UHF communication monopole on a handset is presented to realize a multiuse antenna system for integrated communications and navigation capability. In [17], a dual bands (UHF/S) handset antenna is designed, which consists of a QHA working at S-band (1.9–2.2 GHz) with circular polarization and a monopole antenna at the UHF band (420–520 MHz). The two antennas are arranged coaxially to realize miniaturization.

In this paper, an integrated and miniaturized design of the multimode and multifrequency handset antenna is proposed. A QHA is designed to work at a higher band of 1.98–2.01 GHz and 2.17–2.20 GHz with circular polarization. By substituting each arm with two arms of different lengths and linearly tapered width and loading a helix stub, the QHA is improved to achieve double resonance with increased bandwidth and gain. Moreover, through proper feeding and introducing a quarter-wavelength short-circuit stub, the QHA can also act as a monopole antenna working at a lower band of 0.24–0.7 GHz with linear polarization. The proposed antenna can be applied to the portable multimode and multifrequency handset terminals at VHF/UHF bands.

2. Integrated and Miniaturized Design of Multimode and Multifrequency Antenna at VHF/UHF Bands

2.1. Design of QHA at Higher Band. At higher bands (1.98–2.01 GHz and 2.17–2.20 GHz), the QHA is utilized to realize circular polarization and broad-beam radiation on the upper half-space. The antenna consists of four metal arms wrapped around a thin dielectric cylinder made of PC/ABS. Each arm satisfies the helix parametric equation. If the axis of the cylinder is taken as $+z$ axis, then the upper and the lower line for the helical arm starting from $+x$ axis can be expressed by

$$\begin{cases} x_1 = \dfrac{D}{2}\cos\varphi, \\ y_1 = \dfrac{D}{2}\sin\varphi, \qquad 0 \le \varphi \le \dfrac{2L\cos\alpha}{D}, \\ z_1 = \dfrac{D\tan\alpha}{2}\varphi, \end{cases} \tag{1}$$

$$\begin{cases} x_1 = \dfrac{D}{2}\cos\left(\varphi + \dfrac{2w}{D}\right), \\ y_1 = \dfrac{D}{2}\sin\left(\varphi + \dfrac{2w}{D}\right), \quad 0 \le \varphi \le \dfrac{2L\cos\alpha}{D}, \\ z_1 = \dfrac{D\tan\alpha}{2}\varphi. \end{cases}$$

From the equations above, the structure of the QHA is mainly determined by four parameters: the diameter D of the dielectric cylinder, the pitch angle α, the length L of each arm, and the width w of each arm. The value of D can vary over a wider range. However, a smaller value of D will result in a stronger coupling between the four arms since they are too close to each other, and a larger value of D not only increase the antenna size but also can lead to the change in the radiation pattern on the upper half-space. The value of the pitch angle α can affect the bandwidth, beamwidth, and AR. For larger pitch angle, the number of turns becomes small if other parameters remain unchanged, which can increase both the bandwidth and beamwidth, but the AR also becomes larger and the circular polarization characteristics get worse [18]. The length L of each arm determines the resonated frequency and is set to be equal to $n\lambda_g/4$ in general, where $n = 1, 3, 5, \ldots$ if four arms are open-circuited at the nonfeeding end and $n = 2, 4, 6, \ldots$ if they are short-circuited. It should be noted that the working wavelength λ_g is less than that in free space due to the existence of the dielectric cylinder. In this paper, the four arms of the QHA are open-circuited at the terminal end; therefore, n is an odd number. The greater the value of n, the wider the working bandwidth, and the larger the antenna size. Therefore, $n = 3$ is utilized in this paper to reach a compromise between the bandwidth and the antenna size.

Considering that the QHA works at uplink and downlink mode, each arm of it is replaced by two arms with different lengths [3]. The longer arm with a length of L_1 resonates at 1.98–2.01 GHz, and the shorter one with a length of L_2 at 2.17–2.2 GHz. In addition, the width w of each arm is designed to be linearly tapered from 0.7 mm to 2.2 mm to increase the impedance bandwidth. To improve the antenna gain, a helical stub is innovatively loaded on the main radiator, which behaves as a director and can effectively direct the radiated power to the required upper half-space. By adjusting the lengths L_3 and L_4 of the helix stub and the spacing d from the main radiator, the antenna gain on the upper half-space can be increased. The final

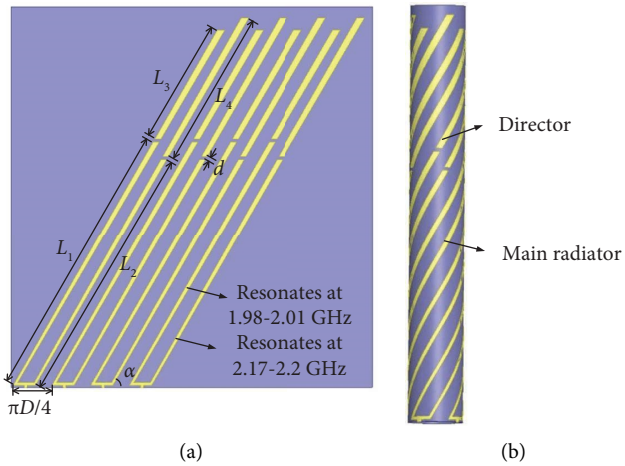

Figure 1: Configuration of improved QHA. (a) Unwrapped model. (b) 3D model.

Table 1: Structure parameters of improved QHA.

Parameter	D (mm)	α (°)	L_1 (mm)	L_2 (mm)	L_3 (mm)	L_4 (mm)	d (mm)
Value	15	60	74	68.7	34	43	0.9

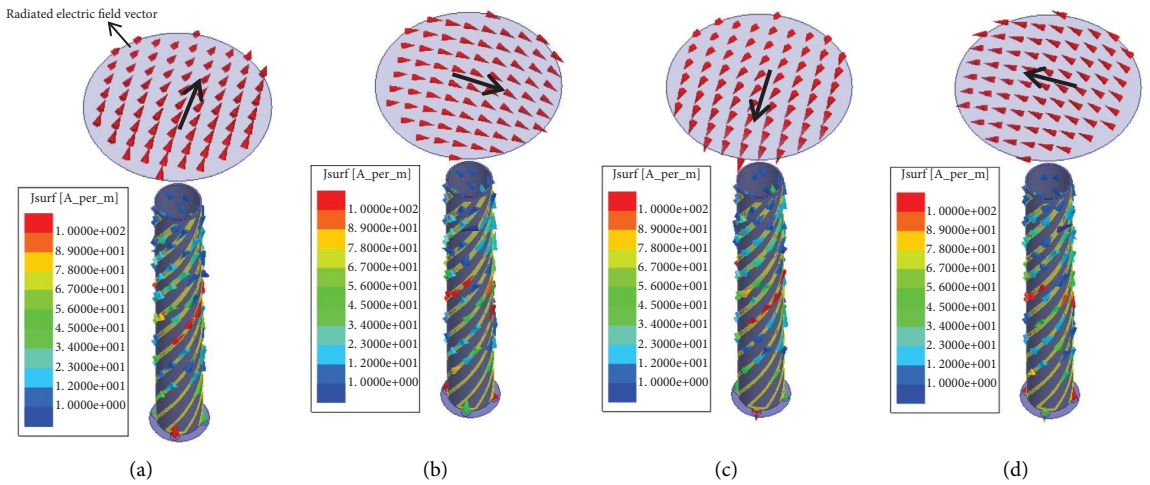

Figure 2: Surface current and radiated electric field distributions of QHA at 1.995 GHz: (a) 0°, (b) 90°, (c) 180°, and (d) 270°.

configuration of the improved QHA is shown in Figure 1, with its structure parameters listed in Table 1.

To realize the circular polarization, the four arms of the QHA are connected to the output ports of a one-to-four power divider and phase shifter at the bottom of the antenna to be fed with equal amplitudes and quadrature phases. In accordance with the analysis in [19], the QHA can be equivalent to two orthogonal small loop-dipole antennas fed in the quadrature phase. Utilizing the field equations of the small loop antenna and dipole antenna, it can be concluded that the electric field components E_θ and E_ϕ are of equal amplitude and have a 90° phase difference; therefore, a circular polarization pattern can be excited. To illustrate this, the surface current distributions on the four arms for different phases of 0°, 90°, 180°, and 270° at 1.995 GHz are simulated and displayed in Figure 2, and the corresponding radiated electric field vectors along the axis direction are also shown in this figure. It is clear that the radiated electric field vectors change with time and rotate in an clockwise manner, which means that a left-hand circular polarization wave is excited.

2.2. Design of Monopole Antenna at Lower Band. At the lower band of 0.24–0.7 GHz, the quarter-wavelength monopole antenna is a good candidate to satisfy the requirement of linear polarization and omnidirectional radiation on the horizontal plane, the design of which is as follows. Firstly, the inner conductor of the feedline at the lower band is connected to the outer conductor of the QHA coaxial feedline; therefore, the feeding current of the lower band will flow along the outer surface of the outer conductor of the QHA feedline; i.e., the outer conductor of the QHA feedline

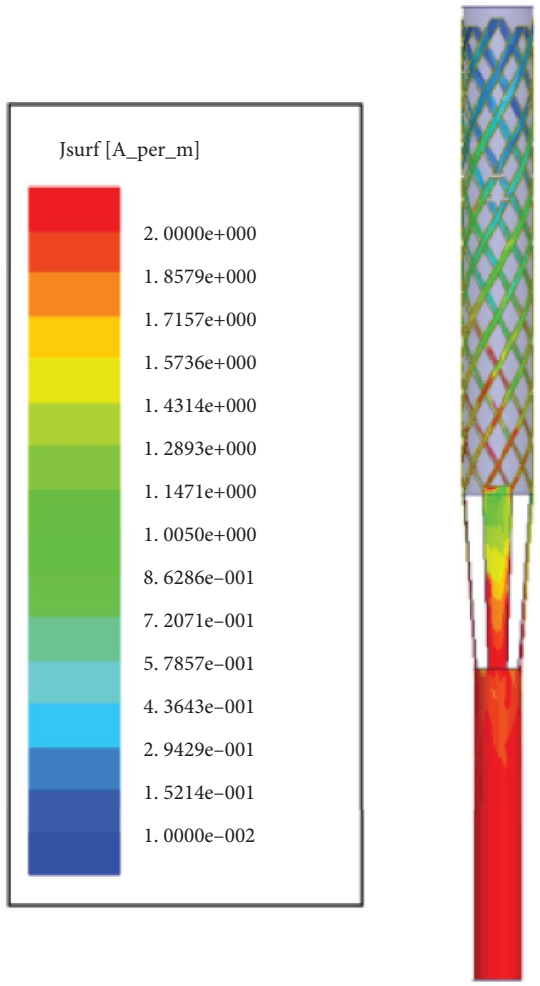

Figure 3: Surface current distribution of monopole antenna.

can act as the radiator of the monopole antenna. Secondly, four short-circuit stubs with a length of quarter-wavelength of the higher band are innovatively introduced to connect the four input ports of the QHA arms with the outer conductor of the QHA feedline. For the higher band, it is equivalent to connect four input ports of the QHA in parallel with a quarter-wavelength short-circuit stub, which therefore does not affect its current distribution due to the quarter-wavelength impedance transforming. For the lower band, the feeding current can be extended from the outer conductor of the QHA feedline to four QHA arms via the short-circuit stubs, i.e., four QHA arms can also be treated as part of the monopole antenna and participate in the radiation of the lower band. In this way, the outer conductor of the QHA feedline, four short-circuit stubs, and four QHA arms, taken as a whole, constitute the radiator of the monopole. With this radiator-sharing technique, the QHA not only works at the higher band with a circular polarization pattern but can act as a monopole antenna working at the lower band with a linear polarization pattern simultaneously. As a result, the size of the antenna can be reduced remarkably since it is unnecessary to design an additional monopole antenna radiator. By adjusting the length of the

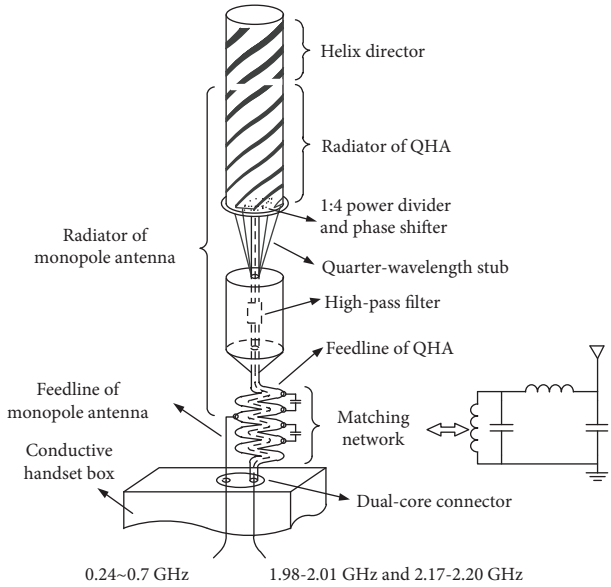

Figure 4: Geometry of the proposed antenna.

QHA feedline, the monopole antenna can resonate at the desiring band. Figure 3 displays the simulated current distribution of the antenna, it is clear that the feeding current flows from the outer conductor of the QHA feedline to four QHA arms via four short-circuit stubs, and it takes the maximum at the feeding port and approximately drops to zero at the end of the QHA arms, which is in agreement with the current distribution of conventional monopole antennas.

Considering that the monopole antenna works over a wider range of frequencies of 0.24–0.7 GHz, it is necessary to design a matching network. As stated above, the inner conductor of the monopole antenna feedline is connected to the outer conductor of the QHA coaxial feedline. At the connection, the QHA feedline is wound into a coil of several turns, which together with the loaded stubs constitutes an LC matching network. By adjusting the length of the loaded stubs, a better matching over the whole operating band can be achieved. In addition, a high-pass filter is inserted in series on the QHA feedline to reduce the mutual coupling between the monopole antenna and the QHA. Finally, by connecting the two feedlines of the monopole antenna and the QHA to a dual-core connector, an integrated and miniaturized multimode and multifrequency antenna is obtained, which can work at both lower and upper bands of VHF/UHF bands simultaneously. The configuration of the proposed antenna is shown in Figure 4.

3. Measured Results and Discussion

The proposed antenna is fabricated with a total length of 228 mm and a diameter of 15 mm as shown in Figure 5. From Figure 6, it is observed that the measured S11 is below −8 dB at the lower band and below −13 dB at the higher band, which means the proposed antenna has good matching over the whole operating band. Figure 7 displays the measured AR, and it is clear that the 3-dB AR beamwidth

(a) (b)

Figure 5: Photograph of the fabricated antenna: (a) front view and (b) upward view.

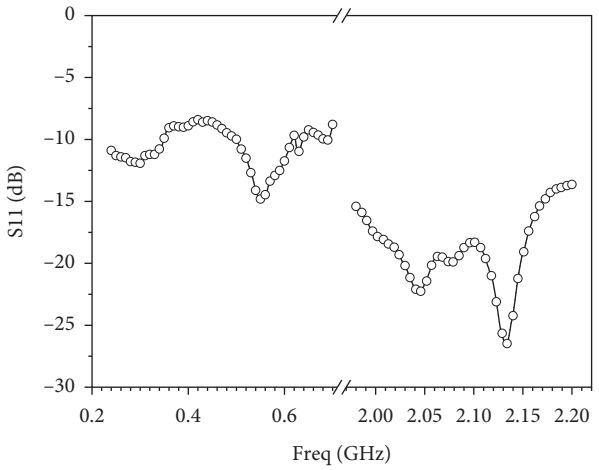

Figure 6: Measured S11.

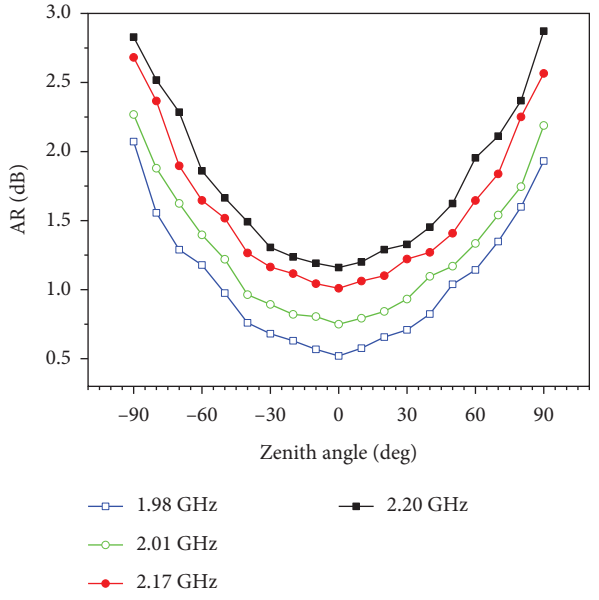

Figure 7: Measured AR.

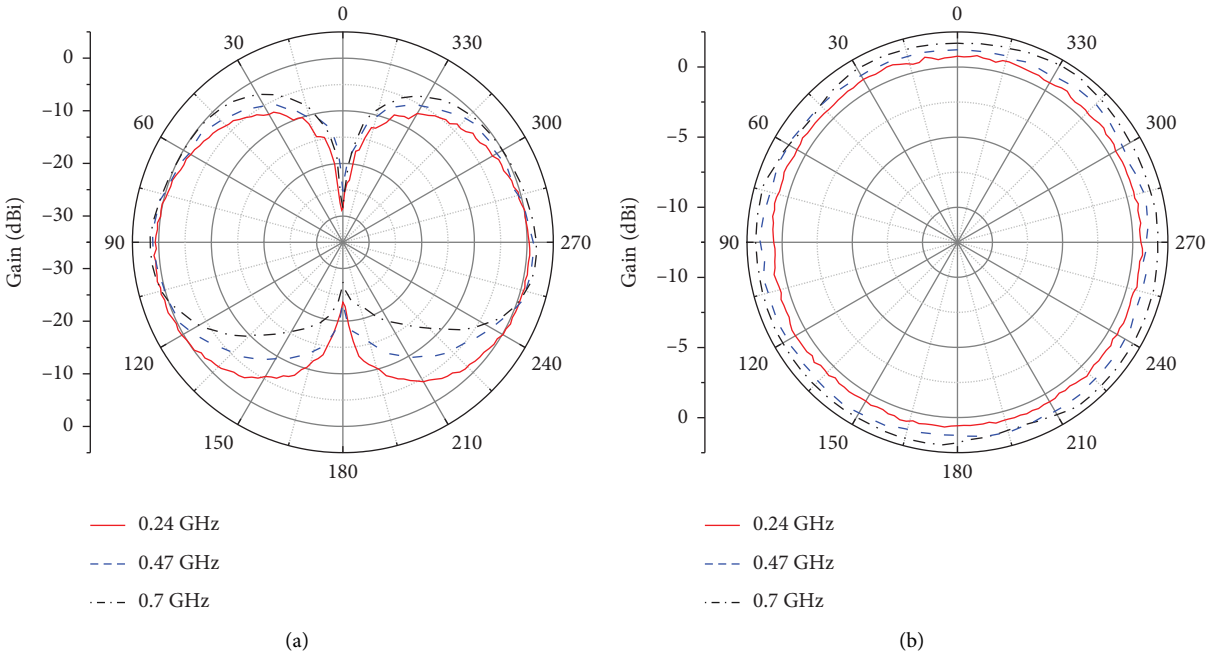

Figure 8: Radiation pattern of the proposed antenna at the lower band: (a) E-plane and (b) H-plane.

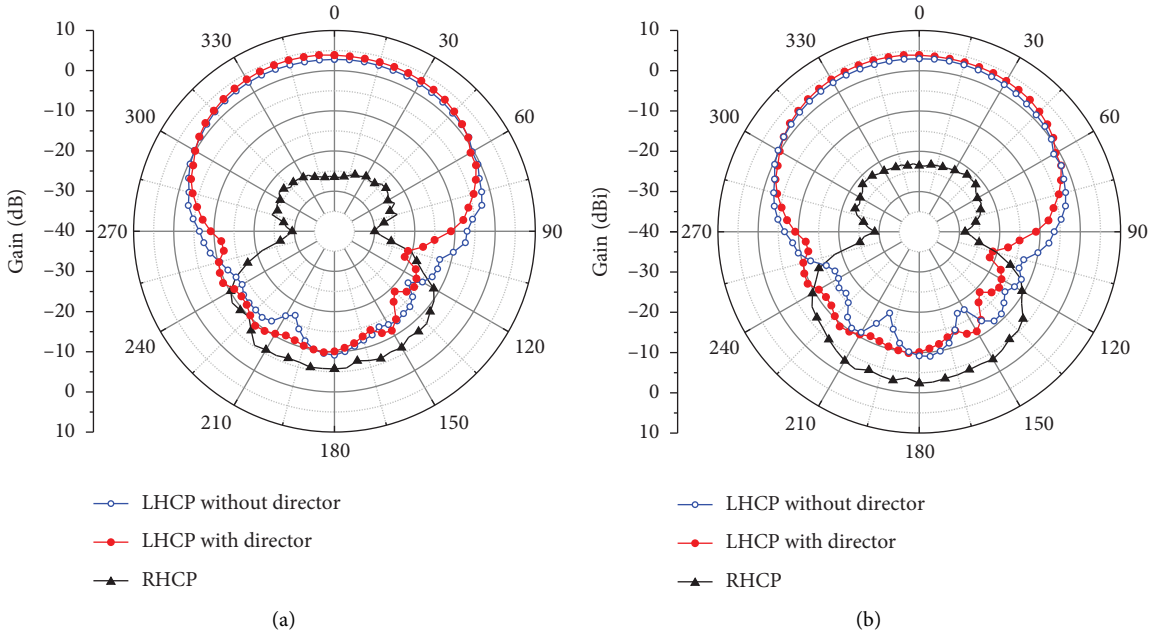

Figure 9: Continued.

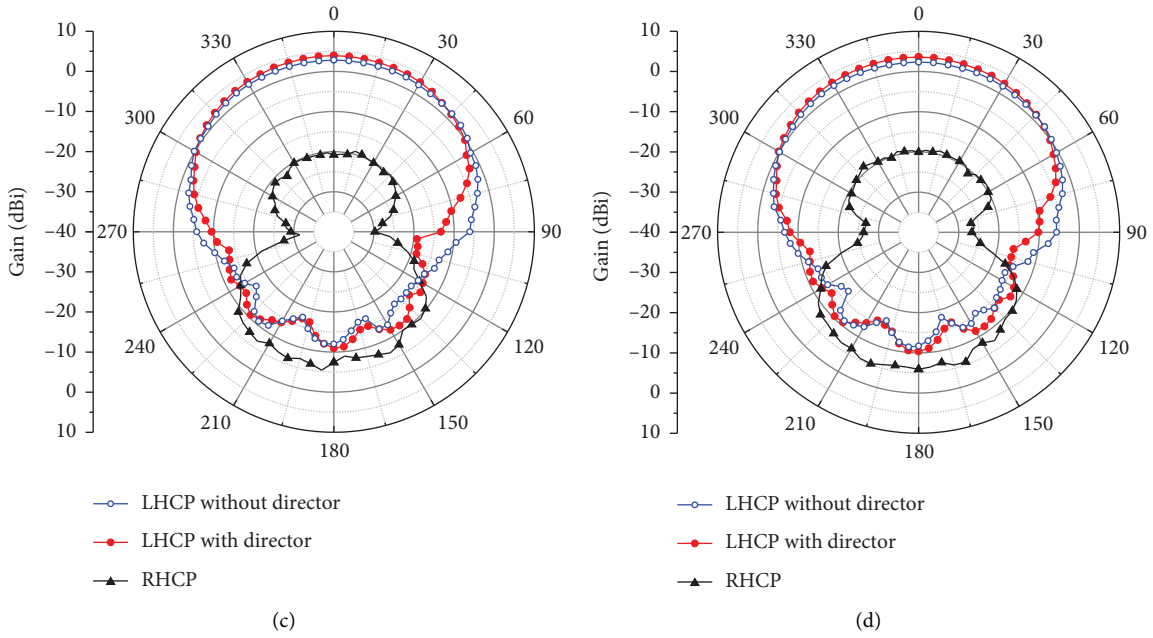

Figure 9: Radiation pattern of the proposed antenna at (a) 1.98 GHz, (b) 2.01 GHz, (c) 2.17 GHz, and (d) 2.2 GHz.

Table 2: Gain at the zenith angle of 0° and 35° for different frequencies.

Frequency (GHz)	Gain at the zenith angle of 0° (dBi)	Gain at the zenith angle of 35° (dBi)
1.98	3.85	2.81
2.01	4.15	2.92
2.17	3.94	3.16
2.20	3.59	2.88

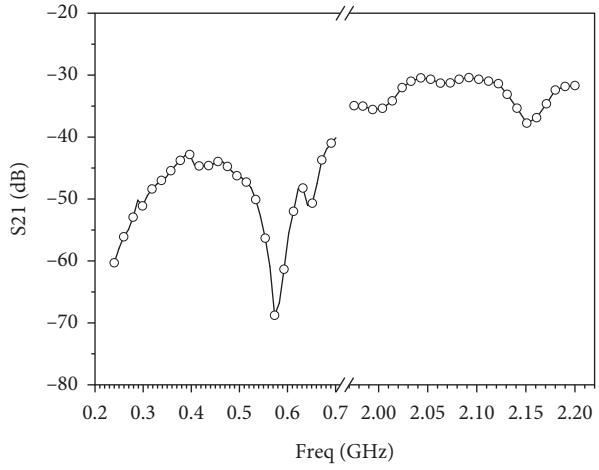

Figure 10: Port isolation of the proposed antenna.

can cover the whole upper half-space, which means good circular polarization characteristics.

The E-plane and H-plane radiation patterns of the proposed antenna at the lower band are shown in Figure 8. As can be seen, the E-plane radiation pattern has the shape of "8" but is tilted upward since the metal enclosure of the handset terminal is not an ideal infinite ground, and the H-plane radiation pattern shows omnidirectional radiation on the horizontal plane.

Figure 9 displays the radiation pattern in the elevation plane at the higher band. The antenna gain can be increased by 1-2 dB with the introduction of a helical director, and higher cross-polarization isolation of more than 20 dB can also be achieved. In Table 2, the antenna gain at the zenith

Table 3: Comparison of the proposed antenna with the previous work.

Ref	Height (mm)	Diameter (mm)	Bandwidth (MHz)	S11	Peak gain	AR
[16]	254	38.1	225~512	Not given	2 dBi	—
			1164~1300 1559~1626	S11 < −2 dB	0.8 dBic	Not given
This work	228	15	240~700	S11 < −8 dB	2.12 dBi	—
			1980~2010 2170~2200	S11 < −13 dB	4.15 dBi	<3 dB for the whole upper half-space

angle of 0° and 35° for different frequencies is listed, which shows that the antenna gain is greater than 2.8 dBi within the zenith angle range of 0° to 35°. The measured isolation between two ports in the lower band and the higher band is displayed in Figure 10. It can be seen that the isolation exceeds 30 dB in both bands, which illustrates a small mutual coupling effect between the monopole antenna and the QHA.

Furthermore, a comparison between the proposed antenna and the reference antenna is listed in Table 3. It can be concluded that the proposed antenna has a higher gain with a smaller size due to the adoption of the director stub and the radiator-sharing technique.

4. Conclusions

An integrated and miniaturized design of the monopole antenna and QHA is proposed, which works at a lower band (0.24–0.7 GHz) with linear polarization and a higher band (1.98–2.01 GHz and 2.17–2.20 GHz) with circular polarization. Measured results show that the proposed antenna has better performance and can therefore be applied to the portable multimode and multifrequency handset terminals at VHF/UHF bands for LTE, self-organizing network, intercom, and satellite communication.

Data Availability

The data used to support the findings of this study are available from the corresponding author upon reasonable request.

Conflicts of Interest

The authors declare that they have no conflicts of interest.

References

[1] X. Zhang, F. Sun, G. Zhang, and L. Hou, "Compact UHF/VHF monopole antennas for CubeSats applications," *IEEE Access*, vol. 8, pp. 133360–133366, 2020.

[2] S. Das and A. K. Iyer, "Design of a highly miniaturized, inherently matched, spherical folded dipole antenna and evaluation of its quality factor," *IEEE Transactions on Antennas and Propagation*, vol. 69, no. 12, pp. 8914–8919, 2021.

[3] Y. D. Yan, Y. C. Jiao, R. Tian, and W. Zhang, "A dual-band circularly-polarized quadrifilar helix antenna," in *Proceedings of the 11th UK-Europe-China Workshop on Millimeter Waves and Terahertz Technologies*, HangZhou, China, September 2018.

[4] G. Byun, H. Choo, and S. Kim, "Design of a dual-band quadrifilar helix antenna using stepped-width arms," *IEEE Transactions on Antennas and Propagation*, vol. 63, no. 4, pp. 1858–1862, 2015.

[5] H. Liu, M. Shi, S. Fang, and Z. Wang, "Design of low-profile dual-band printed quadrifilar helix antenna with wide beamwidth for UAV GPS applications," *IEEE Access*, vol. 8, pp. 157541–157548, 2020.

[6] X. Bai, J. Tang, X. Liang, G. Junping, and J. Ronghong, "Compact design of triple-band circularly polarized quadrifilar helix antennas," *IEEE Antennas and Wireless Propagation Letters*, vol. 13, pp. 380–383, 2014.

[7] A. Abdalrazik, A. Gomaa, and A. A. Kishk, "A hexa-band quad-circular-polarization slotted patch antenna for 5G, GPS, WLAN, LTE, and radio navigation applications," *IEEE Antennas and Wireless Propagation Letters*, vol. 20, no. 8, pp. 1438–1442, 2021.

[8] K. D. Xu, D. Li, Y. Liu, and Q. H. Liu, "Printed quasi-yagi antennas using double dipoles and stub-loaded technique for multi-band and broadband applications," *IEEE Access*, vol. 6, pp. 31695–31702, 2018.

[9] J. W. Kim, T. H. Jung, H. K. Ryu, J. M. Woo, C. S. Eun, and D. K. Lee, "Compact multiband microstrip antenna using inverted-L- and T-shaped parasitic elements," *IEEE Antennas and Wireless Propagation Letters*, vol. 12, pp. 1299–1302, 2013.

[10] J. Kulkarni, C. Y. D. Sim, R. K. Gangwar, and J. Anguera, "Broadband and compact circularly polarized MIMO antenna with concentric rings and oval slots for 5G application," *IEEE Access*, vol. 10, pp. 29925–29936, 2022.

[11] J. Kulkarni, A. G. Alharbi, C. Y. D. Sim et al., "Dual polarized, multiband four-port decagon shaped flexible MIMO antenna for next generation wireless applications," *IEEE Access*, vol. 10, pp. 128132–128150, 2022.

[12] Y. Zhang, X. Y. Zhang, L. H. Ye, and Y. M. Pan, "Dual-band base station array using filtering antenna elements for mutual coupling suppression," *IEEE Transactions on Antennas and Propagation*, vol. 64, no. 8, pp. 3423–3430, 2016.

[13] H. Huang, Y. Liu, and S. Gong, "A dual-broadband, dual-polarized base station antenna for 2G/3G/4G applications," *IEEE Antennas and Wireless Propagation Letters*, vol. 16, pp. 1111–1114, 2017.

[14] R. Wu and Q. X. Chu, "A compact, dual-polarized multiband array for 2G/3G/4G base stations," *IEEE Transactions on Antennas and Propagation*, vol. 67, no. 4, pp. 2298–2304, 2019.

[15] Y. He, Z. Pan, X. Cheng, Y. He, J. Qiao, and M. M. Tentzeris, "A novel dual-band, dual-polarized, miniaturized and low-profile base station antenna," *IEEE Transactions on Antennas and Propagation*, vol. 63, no. 12, pp. 5399–5408, 2015.

[16] P. G. Elliot, E. N. Rosario, and R. J. Davis, "Novel quadrifilar helix antenna combining GNSS, iridium, and a UHF communications monopole," in *Proceedings of the IEEE Military Communications Conference*, Orlando, FL, USA, October 2012.

[17] B. Fan, L. Xu, H. Zhang, and Y. Wang, "Design of a dual (UHF/S) bands antenna handset," in *Proceedings of the 11th International Symposium on Antennas, Propagation and EM Theory (ISAPE)*, Guilin, China, October 2016.

[18] M. Amin and R. Cahill, "Effect of helix turn angle on the performance of a half wavelength quadrifilar antenna," *IEEE Microwave and Wireless Components Letters*, vol. 16, no. 6, pp. 384–386, 2006.

[19] C. C. Kilgus, "Multielement, fractional turn helices," *IEEE Transactions on Antennas and Propagation*, vol. 16, no. 4, pp. 499-500, 1968.